Cell Reports

Article

Evolutionary analysis of gene ages across TADs associates chromatin topology with whole-genome duplications

Graphical abstract

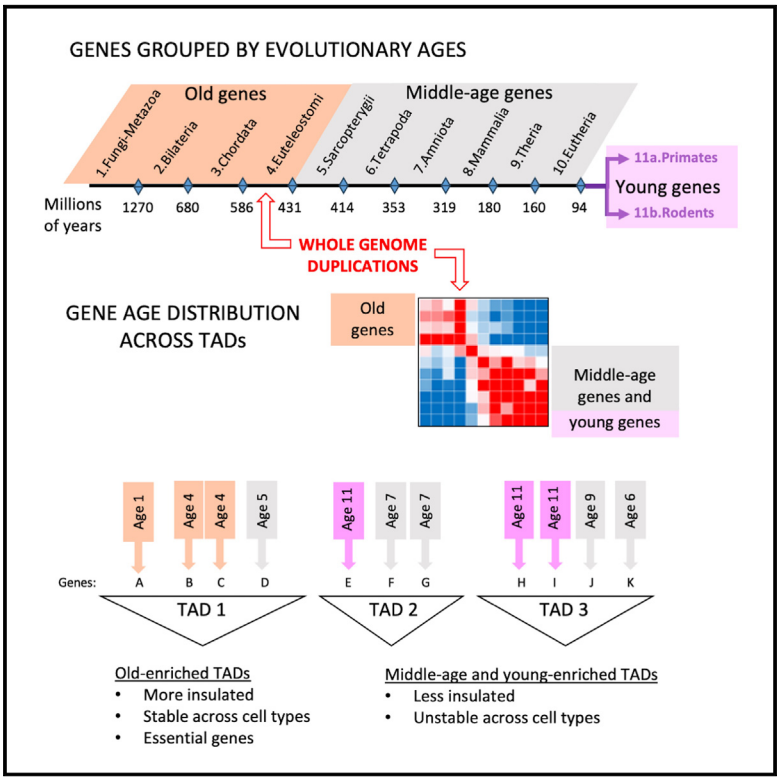

Highlights

- TADs coincide with clusters of genes that are close in their evolutionary age
- Whole-genome duplications mark a transition in gene age co-localization clusters
- Gene age co-localization patterns are associated with TAD insulation
- Young essential genes share TADs and interact with old genes

Authors

Caelinn James, Marco Trevisan-Herraz, David Juan, Daniel Rico

Correspondence

daniel.rico@cabimer.es

In brief

Topologically associated domains (TADs) are considered genomic regulatory modules. James et al. find that genes born before or during the vertebrate whole-genome duplications tend to co-localize in TADs that rarely contain younger genes. They show that TADs enriched in old or young genes have unexpected differential characteristics.

James et al., 2024, Cell Reports *43*, 113895
April 23, 2024 © 2024 The Authors.
https://doi.org/10.1016/j.celrep.2024.113895

CellPress

Cell Reports

CellPress
OPEN ACCESS

Article

Evolutionary analysis of gene ages across TADs associates chromatin topology with whole-genome duplications

Caelinn James,[1,2,7] Marco Trevisan-Herraz,[1,3,7] David Juan,[4,6] and Daniel Rico[1,5,8,9,*]
[1]Biosciences Institute, Newcastle University, Newcastle Upon Tyne, UK
[2]Scotland's Rural College (SRUC), The Roslin Institute Building, Easter Bush, Midlothian, UK
[3]Translational and Clinical Research Institute, Newcastle University, Newcastle Upon Tyne, UK
[4]Institut de Biologia Evolutiva, Consejo Superior de Investigaciones Científicas–Universitat Pompeu Fabra, Parc de Recerca Biomèdica de Barcelona, Barcelona, Spain
[5]Centro Andaluz de Biología Molecular y Medicina Regenerativa (CABIMER), CSIC-Universidad de Sevilla-Universidad Pablo de Olavide-Junta de Andalucía, Seville, Spain
[6]Systems Biology Department, Spanish National Centre for Biotechnology (CNB-CSIC), Madrid, Spain
[7]These authors contributed equally
[8]X (formerly Twitter): @danielrico_bio
[9]Lead contact
*Correspondence: daniel.rico@cabimer.es
https://doi.org/10.1016/j.celrep.2024.113895

SUMMARY

Topologically associated domains (TADs) are interaction subnetworks of chromosomal regions in 3D genomes. TAD boundaries frequently coincide with genome breaks while boundary deletion is under negative selection, suggesting that TADs may facilitate genome rearrangements and evolution. We show that genes co-localize by evolutionary age in humans and mice, resulting in TADs having different proportions of younger and older genes. We observe a major transition in the age co-localization patterns between the genes born during vertebrate whole-genome duplications (WGDs) or before and those born afterward. We also find that genes recently duplicated in primates and rodents are more frequently essential when they are located in old-enriched TADs and interact with genes that last duplicated during the WGD. Therefore, the evolutionary relevance of recent genes may increase when located in TADs with established regulatory networks. Our data suggest that TADs could play a role in organizing ancestral functions and evolutionary novelty.

INTRODUCTION

Recent advances in understanding the modular organization of chromatin are beginning to shed light on the local context within which genes are situated, thanks to the development of chromosome conformation capture (3C) techniques.[1,2] In 3C data, we can see that chromosomes are composed of sets of neighboring genes and regulatory regions that tend to preferentially interact with each other in three-dimensional (3D) space, called topologically associated domains (TADs).

Accumulating data suggest that TAD boundaries could amount to important functional elements, providing a modular system that might enhance the evolvability of genomes. Recent work has shown that synteny breakpoints between different mammals[3,4] and flies[5] are enriched at TAD boundaries. Certain classes of paralog protein-coding genes have been shown to co-localize within TADs and partially share regulatory elements in mammals,[6,7] and clusters of conserved non-coding elements of key developmental genes coincide with TADs in humans and flies.[8] TAD boundaries are evolutionarily constrained,[9] and their deletion is under negative selection.[10,11] Interestingly, a comparison of linkage disequilibrium blocks and TADs revealed that TAD boundaries do not coincide with recombination hotspots, suggesting that recombination might be deleterious at these regions.[12] Taken together, these results indicate that TAD boundaries are conserved but breakable,[13] facilitating genome rearrangements during evolution while preserving intra-TAD functional and regulatory interactions. They also support the integrative breakage model of genome evolution,[14] where chromatin conformation facilitates genome reorganization during evolution.

Evolution is not just driven by rearrangements of the 3D structure of the genome; gene duplication events also play a role in evolution. Most gene duplication events affect genomic regions containing one or a handful of genes, but whole-chromosome and whole-genome duplications (WGDs) can also occur and be important drivers of evolution.[15,16] There has been at least one WGD event (but most likely two) in the ancestor of

This is an open access article under the CC BY license (http://creativecommons.org/licenses/by/4.0/).

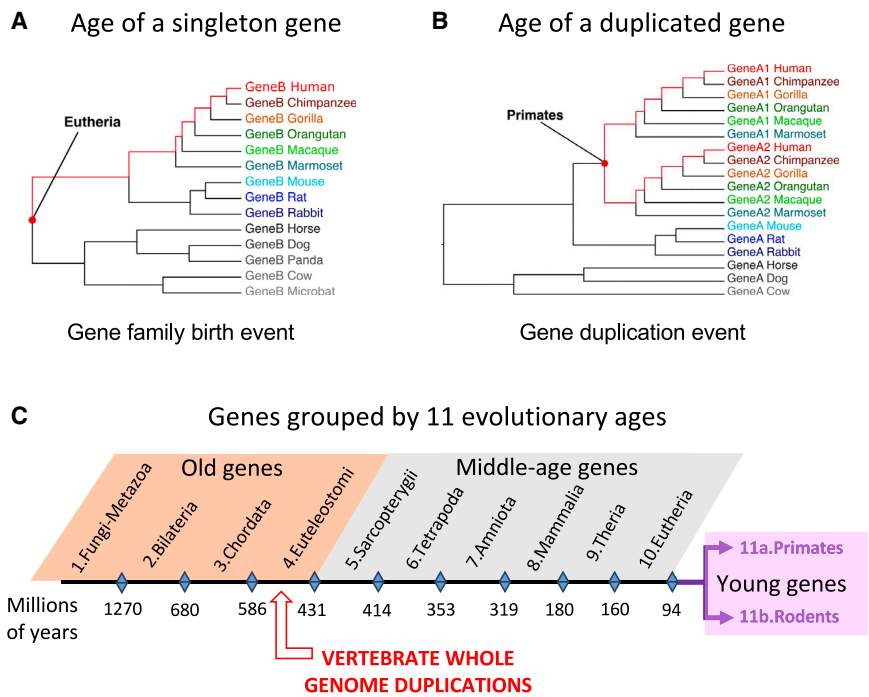

Figure 1. Diagrams showing how gene ages are dated

(A) Toy gene tree illustrating how the gene age corresponds to the last common ancestor for singleton genes.

(B) Toy gene tree illustrating how the gene age corresponds to the most recent duplication node for duplicated genes. As for singleton genes, the gene age indicates the last time a gene was involved in a gene birth event.

(C) Human and mouse genes were grouped in 11 gene age groups (see Table 1 for more details).

vertebrates, and the majority of genes duplicated during this event present in extant vertebrates have not duplicated since.[17–19] More recently, it has been shown that the expansion of many gene families after the WGDs was frequently associated with gene specialization, evidenced by restricted expression and recruitment of novel, tissue-specific regulatory elements contributing to the increase in the regulatory complexity in vertebrates.[20]

Gene duplication events (whether individual genes or WGDs) can allow us to determine the evolutionary "age" of a gene based on its most recent duplication event.[21] The function, expression patterns, and protein-protein interactions of genes are associated with their age, where older genes more frequently perform essential functions, are expressed in more cell types, and show more interactions.[22–24] Evolutionarily old genes are more likely to be essential genes,[24–26] but we still do not understand the role genome architecture may play in the acquisition of essential functions.

Here, we investigated whether protein-coding genes that share a TAD had also originated around the same evolutionary time (and thus share the same evolutionary age). We show how gene age is non-randomly distributed in the human and mouse genomes, where genes within the same TAD tend to have similar gene ages. This gene age co-localization is lost in those TADs containing more inter-TAD interactions in the 3D genome; these TADs also tend to be enriched in young genes. TADs enriched in genes born before or during the WGDs tend to co-localize in TADs that rarely contain younger genes, but when they do, the young genes are more likely to be essential than expected by chance and show more 3D chromatin interactions with older essential genes. Overall, we uncover an intimate relationship between genome architecture and gene evolution, with implications for the emergence of essential functions and the evolution of regulatory circuits in evolutionarily young genes.

RESULTS

Gene ages are not randomly distributed in human and mouse TADs

There are two main ways to define the age of a gene. First, we can define how old a gene is by looking for homologs in other species (with sequence similarity searches such as BLAST) and defining the gene age by the last common ancestor of the species where homologs are found (Figure 1A). In reality, this approach is helpful in estimating the age of the gene family: the age of the root of the phylogenetic gene tree.[21] To estimate the age of each individual gene within a gene family, we can consider when was the last time that the gene was involved in a gene birth event (Figure 1B),[27] where the most common mechanism is gene duplication. In this definition, both parental and daughter genes share the age of the corresponding duplication event.

Human and mouse protein-coding genes were classified into 11 age groups based on each gene's most recent gene birth event[28,29] using gene trees retrieved from Ensembl[30] (Figures 1C; Table 1). Ten age groups correspond to shared ancestors between humans and mice (from Fungi-Metazoa to Eutheria), while the youngest age group in each species corresponds to primate (in humans) or rodent (in mice) gene births; see Table 1 and STAR Methods for more details.

For each age group in humans, we computed the frequencies of finding genes of every other age in the same TAD using TAD maps available from human embryonic stem cells (hESCs; key resources table).[31] We used data from ESCs because they perform some of the oldest functional processes in eukaryotic evolution, such as symmetric and asymmetric cell division, and they themselves constitute one of the evolutionarily older cell types in multicellular organisms.[32–34] To test the significance of this age co-localization, we calculated the p values for the probability of finding gene pairs having each combination of ages (i.e., the probability of obtaining a gene of age *i* in the same TAD by chance when selecting a gene of age *j*). To calculate these p values, we considered the null hypothesis to be the distribution

CellPress
OPEN ACCESS

Table 1. Gene ages used in this study, including the abbreviations used in some figures, number of human and mouse genes in each age group, and the evolutionary time periods covered (in millions of years)

Gene age	Abbreviation	Human genes	Mouse genes	Time periods (Mya)	Age groups
Fungi-Metazoa	FungM	1,135	1,139	1,270	old genes
Bilateria	Bilat	2,975	3,044	1,270–680	old genes
Chordata	Chord	1,184	1,236	680–586	old genes
Euteleostomi	***Eutel***	***8,547***	***8,662***	***586–431***	**old genes *(WGDs)***
Sarcopterygii	Sarcop	190	191	431–414	middle-age genes
Tetrapoda	Tetra	160	156	414–353	middle-age genes
Amniota	Amnta	422	434	353–319	middle-age genes
Mammalia	Mamml	384	377	319–180	middle-age genes
Theria	Thria	526	542	180–160	middle-age genes
Eutheria	Euthr	946	828	160–94	middle-age genes
Primates	PrmtSp	1,255	not applicable	94–0	young genes
Rodents	RdnSp	not applicable	4,713	94–0	young genes

Euteleostomi genes (in bold) correspond to those born during the WGDs. All ages are shared between human and mouse, except primates (primates specific, or PrmtSp, in human) and rodents (rodent specific, or RdnSp, in mouse). See STAR Methods and key resources table for details.

of these probabilities when randomizing the ages of the genes (and hence across TADs; see Figures 2A and S1 and STAR Methods). To visualize the p values, we generated a matrix showing the probability of finding each combination of gene ages (Figure 2B).

The age co-localization results show that gene ages are not distributed randomly in the TADs of the human genome (Figures 2B, left, and S2). For the sake of simplicity, we merged gene ages into three major groups: old (genes not duplicated since the WGDs with Euteleostomi or older ages), middle-age (from Sarcopterygii to Eutheria) and young (primates, or rodents in the case of mouse; see Figure 1C for details) genes. Surprisingly, our analysis shows a clear co-localization pattern according to two gene age groups. The old genes are significantly co-localized within the same TADs. However, they share TADs with middle-aged and young genes less often than expected by chance. In contrast, we see significant TAD co-localization of young and middle-aged groups (Figure 2B).

To further test the observed pattern of gene age co-localization, we randomized the age labels of each gene and repeated the analysis. We observed no age co-localization when age labels were randomly assigned (Figures 2B, right, and S3). This suggests that the co-localization effect we saw between old gene ages (Fungi-Metazoa to Euteleostomi) on the one hand and between middle-aged to young genes on the other hand was not random but instead an effect of genome structure.

To assess whether this result is ESC specific or depends on the TAD definitions used (which can vary depending on the TAD-calling method),[1,35] we performed the same analysis using independently defined TAD maps from different cell types: human B cell-derived lymphoblastoid GM12878 cells (derived from the highest-resolution HiC data in humans to date),[36] monocytes, neutrophils, and naive CD4 T cells[37] (key resources table). In all these cases, two very similar age co-localization groups were also observed (Figures S4 and S5).

Within the group of old genes (see Figure 1C), Euteleostomi genes (or ohnologs) are the most recent, corresponding to gene duplications that resulted from WGDs that occurred at the origin of the ancestral vertebrate genome.[17–19] If the marked gene age co-localization we observed in humans is associated with the gene birth events before and after the WGDs, then we would expect to see a similar pattern in the mouse genome (as they share all the gene ages until the primates-rodents split).

Therefore, we performed the same analysis using mouse genes and TADs from mouse ESCs (derived from the highest-resolution HiC data in mouse to date[38]; key resources table). Interestingly, a very similar significant pattern was observed in the mouse (Figure 2B, bottom left) that disappeared when the age labels were randomized (Figure 2B, bottom right). It is particularly remarkable that primate and rodent genes show the same pattern, although they represent independent gene birth events.

In summary, the results in both species show that there is a major transition in the TAD co-localization patterns prior to Sarcopterygii, coinciding with the time when the two rounds of WGDs are thought to have occurred.[19]

Gene age co-localization is stronger in TADs than in fixed-size partitions of the human genome

As genes within the same TAD are close to each other, we need to consider that the observed co-localization of gene ages could be TAD independent. To test this alternative hypothesis, we divided the human genome into windows of fixed size, using different sizes (ranging from 20 kb to 50 Mb), and repeated the analysis for each window size (Figure 3). For each window size, we generated a corresponding matrix of p values and generated a heatmap. A visual comparison of the results obtained suggests that fixed windows in the size range of TADs (300 kb to 1 Mb) show similar patterns of co-localization but are less evident than real TADs (Figure 3).

To quantitatively compare the results of different windows and real TADs, we calculated the similarity (Euclidean distance) of each observed matrix of p values to an extreme pattern of co-localization where genes perfectly cluster in either the four older (Fungi-Metazoa–Euteleostomi) or seven younger

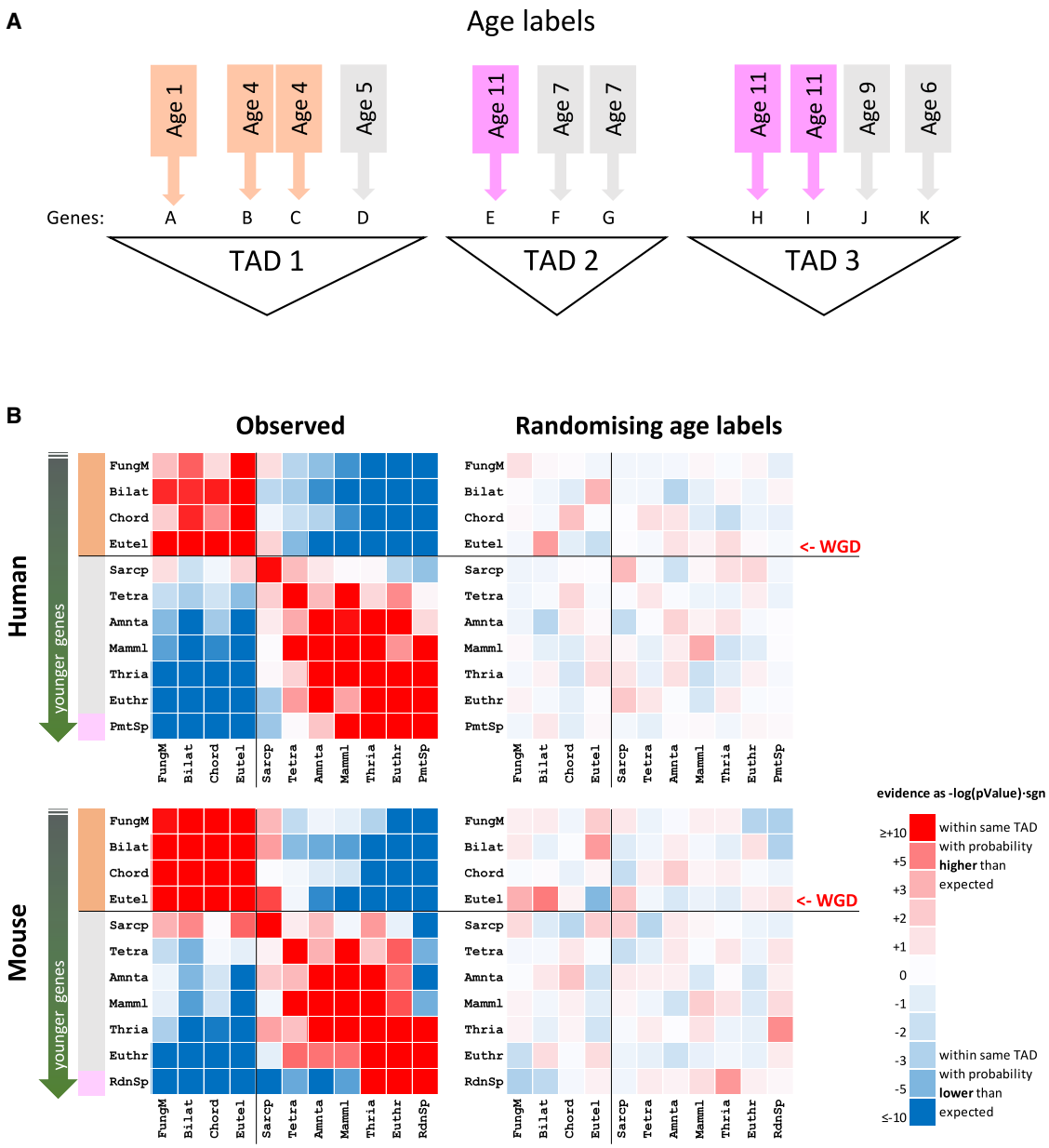

Figure 2. Genes co-localize by age in TADs

(A) Cartoon representing three TADs and their genes. In the co-localization analysis, genes are kept in their original locations, and gene age labels are randomly relocated.

(B) Representation of the matrices displaying the evidence that genes with any combination of two ages are found together in the same TAD by using the natural cologarithm of the p value, using a positive (negative) sign when this is higher (lower) than expected. Increasing intensities of red (blue) show increasing evidence that the combination is found together more often (less often) than expected by chance, with white representing that the match found is exactly as expected by chance. See Table 1 for the correspondence between abbreviated and full gene ages. The color legend next to the abbreviated age names indicates the three gene age groups depicted in Figure 1C; the gene age corresponding to the whole-genome duplication (WGD) is indicated with black horizontal and vertical lines. Left: observed p values for human and mouse. Right: representative results of the same operation after randomizing 100 times the age labels of each gene (so each age group keeps the same number of genes but just assigned randomly).

(Sarcopterygii–primates) age groups. The Euclidean distance between two numeric matrices is a measure of the straight-line distance between their respective points in the multidimensional space defined by the matrices' rows or columns (STAR Methods). This approach showed that the matrix with co-localization p values obtained with the TADs has a shorter Euclidean distance (meaning a higher similarity) than any fixed-size windows, indicating that the co-localization pattern is stronger in TADs. Therefore, the observed results cannot be simply explained by the linear proximity of genes.

CellPress
OPEN ACCESS

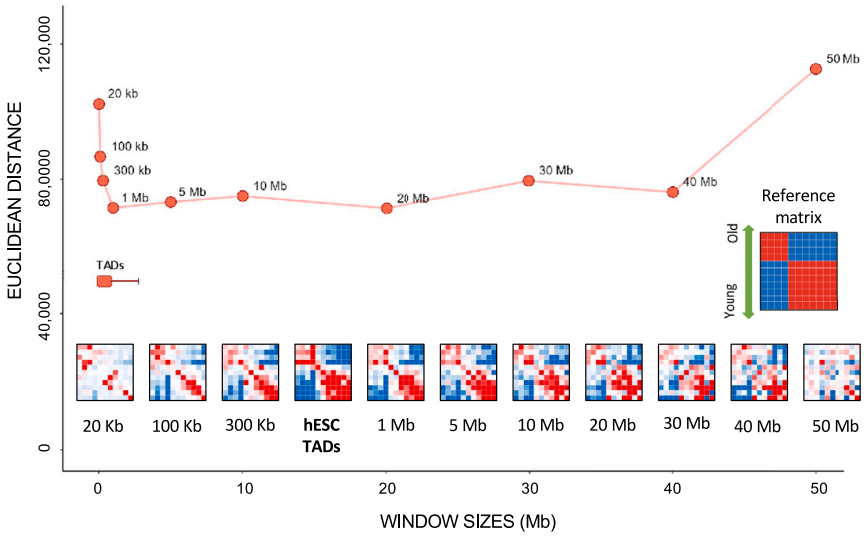

Figure 3. Comparison of co-localization of genes of different ages in both TADs and fixed-size windows

Each heatmap at the bottom represents the gene age co-localization p values (see color legend and more details in Figure 2) obtained using the fixed-size windows of the indicated sizes—from 20 kb to 50 Mb. The heatmap with p values obtained with the hESC TADs (same as in Figure 2) is included for comparison. The points in the graph show the quantitative comparison of the p value matrices with a reference matrix (top right) that represents an extreme two-group co-localization pattern. The y axis indicates the Euclidean distance of each real p value matrix to this reference. The x axis represents the size of the fixed-size window used (and the ranges of sizes for TADs).

We found that the 20 Kb and 50 Mb windows had the highest Euclidean distances. In the case of the 50 Mb window, the window covers the whole chromosome for some of the shorter chromosomes, and so the co-localization pattern that emerges is more likely representing the co-localization of gene ages by chromosome. In the case of the 20 Kb window, the window is so small that it does not capture many genes at once and thus does not generate many meaningful comparisons.

Gene age co-localization patterns are related to TAD insulation

TAD boundaries can show different degrees of insulation[39]: the higher the insulation, the fewer inter-TAD interactions are observed (Figure 4A). Boundaries with higher insulation are generally associated with more CTCF binding[40,41] and are thought to prevent undesired enhancer-promoter interactions between different neighboring regulatory programs.[42] To further investigate the connection of gene age co-localization with TAD structure, we studied its relation to the insulation of TADs. For this, we used the TAD boundary insulation scores calculated by Gong and co-workers[43] using the high-resolution HiC data[36] of the human lymphoblastoid cell line GM12878 (key resources table). We calculated a TAD insulation score by averaging the insulation scores of their boundaries and then divided the TADs into five quintiles based on their insulation (from very low to very high; Figure 4B). We found that the gene age co-localization pattern was different depending on the TAD insulation strength, which was almost lost in the two groups with the lowest insulation strength (Figure 4B). Interestingly, the strongest two-group pattern was observed in those TADs with intermediate insulation. High and (especially) very high show a stronger co-localization pattern near the diagonal, showing a higher resolution of the gene age co-localization and suggesting different gene birth dynamics.

The gene age co-localization patterns can also be affected by other factors that might vary among these five groups of TADs, such as the size of the TADs or their number of genes. Therefore, we decided to investigate the characteristics of TADs with differing insulation strengths. We observed that more insulated TADs tend to be significantly smaller ($p = 4.33 \times 10^{-12}$, comparison between the very low and very high insulated groups; Figure 4C) but have a significantly higher gene density ($p < 2.2 \times 10^{-16}$; Figure 4D). Next, we analyzed how the youngest genes born during the primates lineage varied among the TAD insulation groups: Young genes are relatively more enriched in more insulated TADs ($p < 2.2 \times 10^{-16}$, Figure 4D). In summary, these results show that the more insulated TADs are, the more gene density they have in general, but they also have a relatively higher proportion of young genes. The combination of these properties probably contributes to the differences in gene age co-localization patterns associated with the TAD insulation strength.

TAD boundaries can be stable or conserved across many cell types or can be restricted to one or a few cell types. By analyzing the TADs in 37 human cell types, it has been shown that the TAD boundaries that are more stable across cell types are associated with higher evolutionary constraints, CTCF binding, and housekeeping genes.[9] Therefore, to further study the observed conservation of the co-localization pattern in different cell types, we investigated if human TAD stability[9] (key resources table) was associated with different proportions of gene ages. We consider TADs to be stable if their boundaries are shared among at least 5 cell types, while the boundaries of unstable TADs are shared by 4 cell types or less, as this threshold splits the distribution into two groups of similar size (see STAR Methods). We compared the ratio of old-depleted TADs (those that contained less than 10% of old genes) between stable and unstable TADs and found that unstable TADs have a significantly higher ratio of old-depleted TADs (Figure S6). In other words, TADs unusually rich in young (primate) and middle-age genes tend to be less stable across cell types.

Essential young genes are associated with TADs enriched in old genes

Evolutionarily old genes are more frequently expressed across cell types and are more often classified as "essential" than younger genes.[25,26] Essential genes are required for growth, development, and reproduction, either at the cellular level or at the whole-organism level,[25,44] and loss of function of these

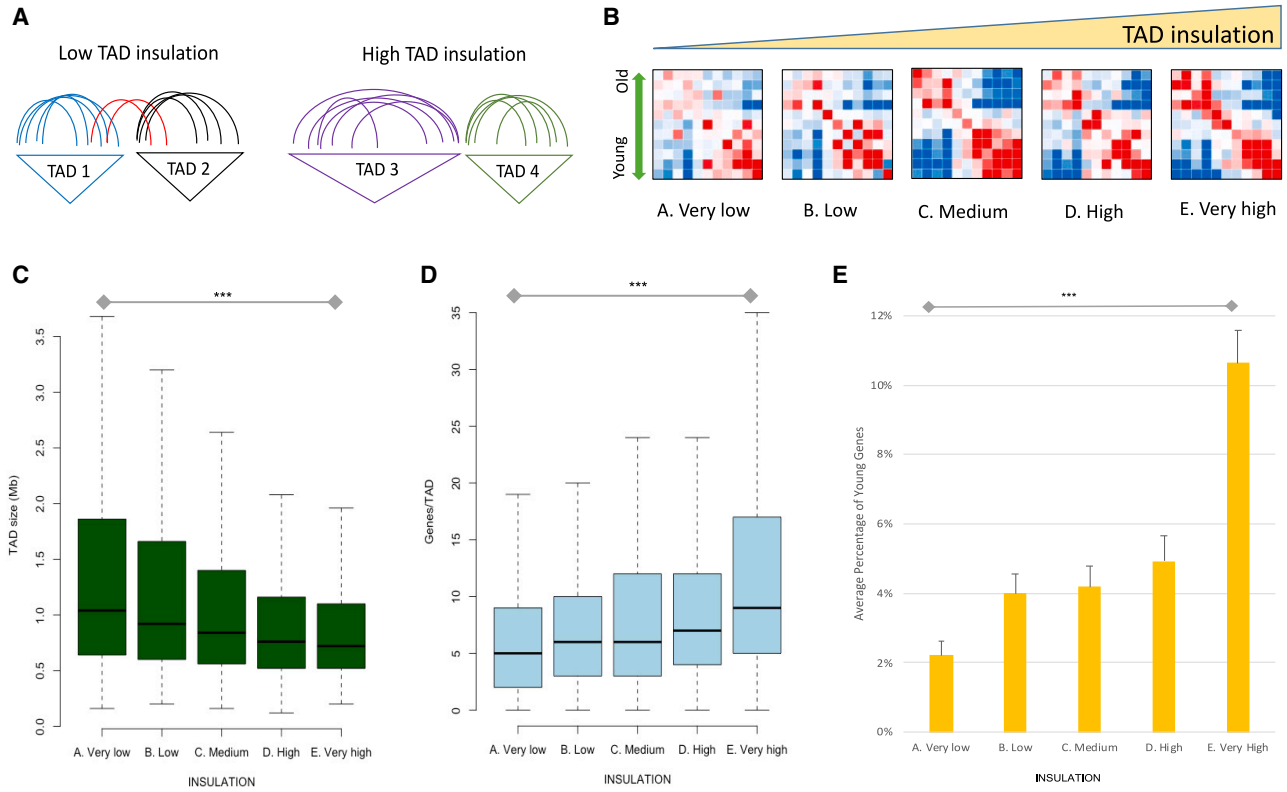

Figure 4. TAD boundary insulation is associated with gene age co-localization patterns

(A) Cartoon illustrating TAD boundary insulation; the more inter-TAD 3D interactions that occur, the lower the insulation strength between two neighboring TADs.

(B) Co-localization p values obtained for the five groups of TADs of GM12878 lymphoblastoid cells, based on their boundary insulation strength. For details, see Figure 2 and its legend.

(C) TAD size distributions for the five insulation groups of TADs in (B).

(D) Distributions of the number of genes per TAD insulation group.

(E) Percentage of young (primates) genes for the five TAD insulation groups. Error bars indicate the standard errors.

Significance of Wilcoxon's (C and D) and chi-squared (E) tests: ***$p < 0.001$.

genes can compromise the viability or fitness of the organism.[25,26] It is assumed that the reason that evolutionarily older genes are more likely to be essential is due to older non-essential genes gradually being removed by evolution. However, it is still unclear how some young genes become essential. We therefore chose to investigate the differences in TAD environments between essential young genes and non-essential young genes to understand whether TAD location may influence the probability of young genes becoming essential.

We examined how the proportion of essential genes in a TAD varied depending on the ages of the genes within the TAD. We used the database of Online Gene Essentiality[44] (key resources table) to determine whether each gene was essential or not. As expected, as a TAD increases in the proportion of young genes, it decreases in the proportion of essential genes, while the opposite was true for the proportion of old genes (Figure 5A).

Next, we investigated if young essential genes were enriched in TADs with other young genes or with older ones. For this, we focused our analyses on two types of TADs: "old-enriched TADs," in which at least 50% of the genes were old (Euteleostomi or older; Figure 1C), and "young-enriched TADs," in which at least 50% of the genes were primate (in human) or rodent (in mouse). We grouped the genes in these TADs depending on whether they were young genes in young-enriched TADs, young genes in old-enriched TADs, old genes in young-enriched TADs, or old genes in old-enriched TADs and calculated the proportion of genes in each group that were essential (Figure 5B). We then carried out chi-squared tests between each group to determine if there were any significant differences.

We found in both the mouse and the human dataset that young genes in young-enriched TADs were less likely to be essential than young genes in old-enriched TADs (humans: $p = 5.54 \times 10^{-3}$, mice: $p = 1.29 \times 10^{-3}$), while the frequency of essential old genes was similar in young-enriched and old-enriched TADs (humans: $p = 1$, mice: $p = 4.49 \times 10^{-2}$). These data suggest that the age of neighboring genes can help determine whether or not a young gene is essential or functionally important, while for old genes, the age of the neighboring genes does not seem to be informative (Figure 5B).

Essential young genes show more 3D interactions with old genes and other essential genes

The enrichment of essential young genes in old-enriched TADs could be associated with its incorporation with evolutionary

CellPress
OPEN ACCESS

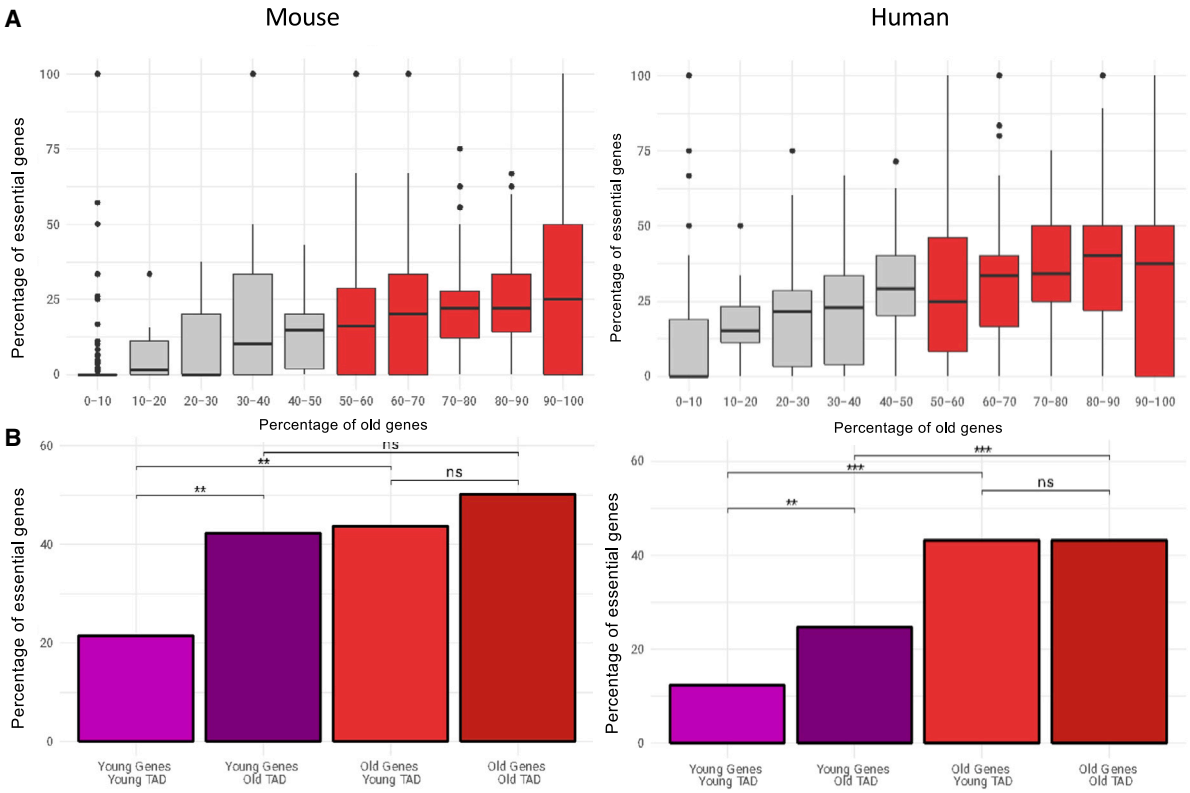

Figure 5. Different proportions of young genes, old genes, and essential genes across TADs in mice and humans

(A) Variation of the percentage of essential genes in comparison to the percentage of old genes. Left: mouse; right: human.

(B) Percentage of essential genes across four gene groups—young genes in young-enriched TADs, young genes in old-enriched TADs, old genes in young-enriched TADs, and old genes in old-enriched TADs. Left: mouse; right: human. The asterisks indicate the p values when carrying out chi-squared tests between the different groups. Significance of chi-squared tests: *p < 0.05, **p < 0.01, and ***p < 0.001 (ns, non-significant).

older regulatory networks, which would result in an increased number of chromatin 3D interactions with older genes. To explore this hypothesis, we analyzed publicly available high-resolution promoter-capture HiC (PCHi-C) networks from mouse[45] and human cells[37] (key resources table). Each network consists of nodes that represent the PCHi-C fragments and edges that represent their interactions.[46] To compare the interactions of young essential genes with those of young non-essential genes, we constructed a subnetwork from the PCHi-C data in each species, keeping only interactions that involve nodes with lineage-specific genes (STAR Methods). From there, the subnetwork was divided into two further subnetworks: one subnetwork where every pair of interacting nodes contained a node with an essential young gene and a second subnetwork where every pair of interacting nodes contained a node with a non-essential young gene. For both subnetworks, we looked at the age and essentiality of the interactors (Figure 6A).

We found that essential young genes have more chromatin interactions with old genes than non-essential young genes in both mice ($p = 7.7 \times 10^{-90}$) and humans ($p = 9.2 \times 10^{-21}$). Essential rodent and primate genes also showed significantly higher interactions with other essential genes, and a similar trend was observed when we looked at interactors that were both old and essential (Figure 6A). These results suggest that, independently of any definition of TADs, 3D interactions with old and/or essential genes are associated with a higher probability of a young gene being essential. Although we do not know how many of these physical interactions are actually regulatory, these enrichments suggest that young essential genes have a higher probability of being co-regulated with old and/or essential genes.

Zinc-finger protein 141 (ZNF141) is a representative example of a young human essential gene (based on CRISPR-Cas9 screening data)[44] located in a TAD rich in old genes; out of the 27 genes in the TAD, 22 (81.5%) are aged Euteleostomi or older (Figure 6B). This TAD is in the telomeric region on chromosome 4p16.3 and contains another 4 essential genes, three of which are directly interacting with ZNF141 in hESC DNAse HiC data[31]: MAEA (Bilateria), GAK (Euteleostomi), and ZNF721 (primates). Interestingly, mutations in ZNF141 have been shown to be associated with postaxial polydactyly type A malformation characterized by well-formed functionally developed 5th digit duplication in hands and/or feet.[47]

DISCUSSION

Genes co-localize in the genome by age

Previous works have shown that synteny breakpoints in mammals[3,4] and flies[5] tend to be located near TAD boundaries.

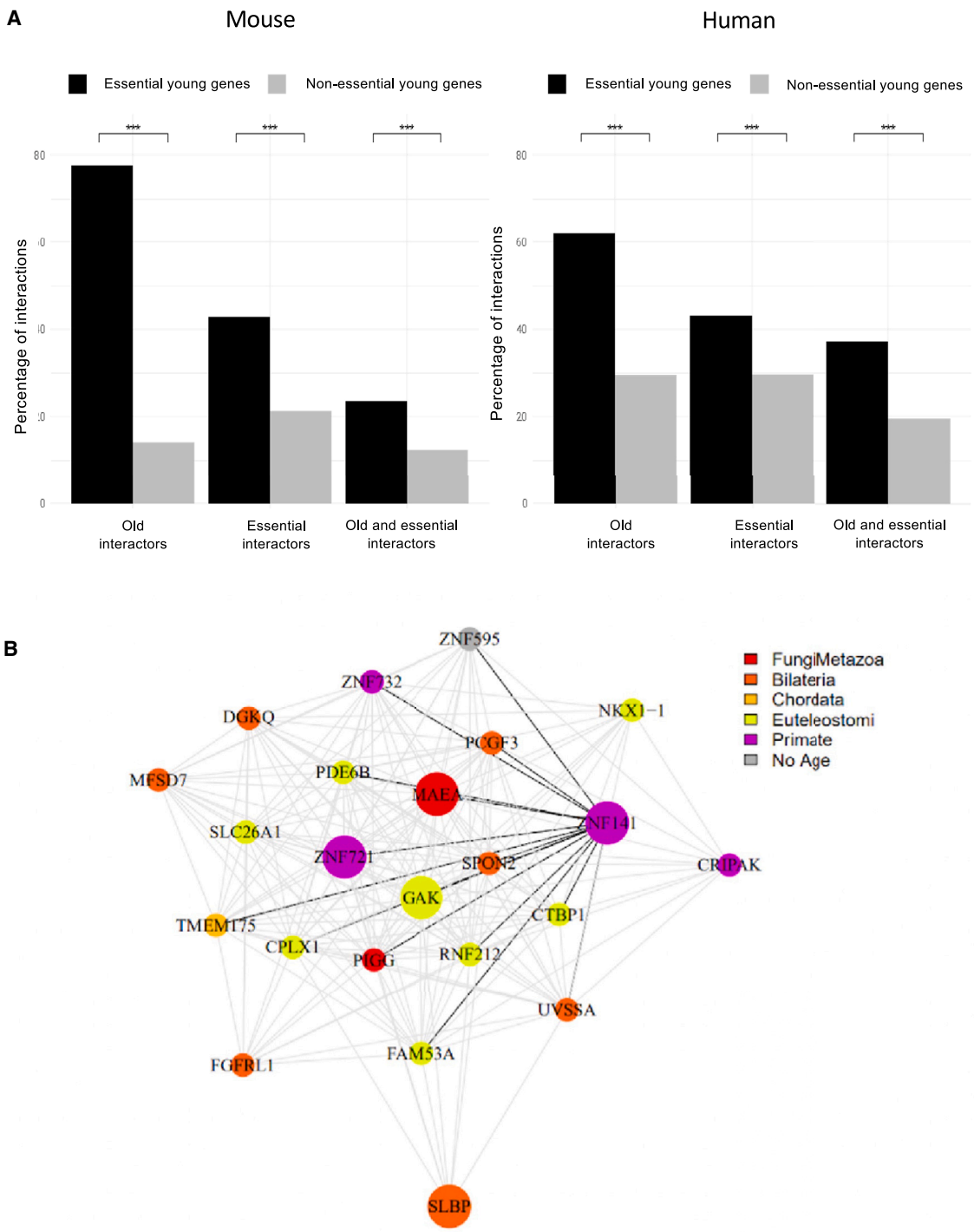

Figure 6. Young essential genes interact more frequently with old and essential genes

(A) Comparison of PCHiC interactions with old, essential, and old and essential interactors for essential rodent and non-essential rodent genes in mouse ESCs (mESCs; left) and essential primate and non-essential primate genes in human CD8 T cells (right). Asterisks indicate that p values for the chi-squared tests were all below 0.001.

(B) HiC interaction network for the TAD containing ZNF141. Nodes represent genes within the TAD, while the edges represent the interactions between the genes. Essential genes are represented with a large node, while non-essential genes are represented with a small node. Black edges represent interactions involving ZNF141. The age of a gene is represented by the color of the node.

Although we still do not know what are the underlying causes that explain these observed correlations, it is tempting to speculate that regulatory or functional interactions within some TADs might be important to maintain. Indeed, other independent works have reported that TAD boundaries show evolutionary constraints.[9–11]

Here, we have found that the TADs in human and mouse genomes coincide with clusters of genes that are close in their evolutionary age. The local expansion of duplicating gene families is probably a key factor contributing to the co-localization of younger genes. It is possible that the structure of TADs that are rich in old genes is under negative selection and that the birth of new genes there is detrimental. This might have been important at least right after the WGDs and then promoted by the local expansions of genes afterward, which tend to accumulate in error-prone late-replicating regions of the genome.[28] Of course, this observation does not imply any causative relationship between the WGDs and TAD structure, as many other factors could have contributed to these gene age co-localization patterns. However, our results suggest this is an intriguing hypothesis that deserves to be investigated in the future.

Ohnolog pairs have been shown to exhibit higher spatial proximity in 3D nuclear organization than other paralog pairs.[48] Taken together with our own data, these observations suggest that the constraints of the WGDs could have influenced the genome architecture in mammalian genomes. Our results comparing the co-localization of gene ages in TADs and windows of fixed sizes indicate that the TAD structure may potentially be playing a role in the observed gene age distribution. These results show the gene age co-localization is stronger when using TADs than when we used fixed-size windows of different sizes, suggesting that there is a significant association between TAD locations and gene age distribution in the genome. As the main difference we observe is between genes born during the WGDs (Euteleostomi) or earlier, we can speculate that TAD structure could have helped to maintain regulatory interactions among genes within old-gene-rich TADs and buffer, to some extent, the effect of regulatory interactions with younger genes. However, it is important to note that we only explored chromatin physical interactions, and future perturbation experiments will be needed to determine which ones are actually regulatory.

Another possibility is that the lower rates of mutations and copy-number variants in early-replicating TADs, rich in old genes, reduce the probability of genes being born there, independently of negative selection biases. Early-replicating TADs are expected to have more efficient DNA repair[49] to reduce the probability of having damaging mutations; the low frequency of young genes in these TADs there might be a secondary effect of a lower mutation rate in these regions. Future availability of TADs in a wider diversity of species will allow us to investigate the conservation of these TADs and their chromatin interactions.[50–52]

Interestingly, we noticed that gene age co-localization patterns vary depending on TAD insulation and that the co-localization is actually not observed in lowly insulated TADs. In contrast, very highly insulated TADs are more enriched in recently born genes, and genes there tend to co-localize more with genes born immediately before or after them. This could reflect a more dynamic evolutionary history in these TADs, an interpretation that is compatible with the higher gene density that we have observed on them. We also found that more insulated TADs tend to be smaller despite showing higher gene density, suggesting that it might be more complicated to insulate larger regions. A recent comparative analysis of TADs in 4 different primates and 4 different rodents identified ultraconserved TADs shared by humans and the other 7 species.[52] Interestingly, these ultraconserved TADs show higher insulation strength and contain genes with cell-type-specific patterns.

The essentiality of genes varies by gene age

The enrichment of young essential genes in old-enriched TADs could be associated with different factors: the higher probability of the chromatin in these TADs to be open, functional relationships with the same essential processes where their neighbors are involved, or new regulatory and/or structural roles keeping the integrity of the 3D structure. Indeed, the potential ability of TADs to encapsulate regulatory environments might allow them to preserve, and might protect them from, the rise of other, younger environments.

Some of these young essential genes could indeed have originated from parental genes that were already essential in the ancestral species; in this case, the essentiality itself would be older than the gene age. Moreover, enhancers have been shown to be a possible substrate for the origin of new genes,[53–55] and it is also possible that the essentiality retrieved from CRISPR screens is actually capturing the essentiality of the regulatory role of the genomic regions. Indeed, promoters with enhancer function of interferon signaling response have been shown to be more conserved than other, non-enhancer genes belonging to the same pathway.[56]

Conclusion

Ultimately, our findings have a simple but very important implication: TADs can be classified by the age of their genes. This can be useful to study the evolution of different biological processes, such as regulatory modules of development, cell-type ontogenies, or cancer. Here, we explored the relationship between TADs, gene age, and gene essentiality, showing that young essential genes tend to be located in TADs rich in genes that are older than them. This could help with prioritizing the study of genes of unknown function by taking into account the age of their neighbors.

Limitations of the study

The estimation of gene ages of human and mouse genes depends on the quantity and variable quality of species genome assemblies and gene annotations available, as well as the quality of automatic gene tree reconstructions. Initiatives such as the Earth Biogenome Project[57] will help to have better species coverage and finer resolution of gene ages. However, this will come with additional computational challenges associated with gene tree reconstructions.

This study is also limited to the HiC-derived TAD datasets from humans and mice that were generated by different laboratories

and processed in different ways. Analyzing more TAD data from HiC uniformly processed and harmonized for different cell types across more mammalian species, together with the availability of age data for the different species in the future, will enable us to explore whether the results are consistent across more cell types and species.[50–52]

STAR★METHODS

Detailed methods are provided in the online version of this paper and include the following:

- KEY RESOURCES TABLE
- RESOURCE AVAILABILITY
  - Lead contact
  - Materials availability
  - Data and code availability
- METHOD DETAILS
  - Dating ages in genes
  - TAD maps used in age co-localization analysis
  - Gene essentiality data
  - Promoter-capture HiC (PCHi-C) networks
- QUANTIFICATION AND STATISTICAL ANALYSIS
  - Gene age co-localization analysis
  - TAD insulation
  - TAD stability across cell types
  - Enrichment of essential genes

SUPPLEMENTAL INFORMATION

Supplemental information can be found online at https://doi.org/10.1016/j.celrep.2024.113895.

ACKNOWLEDGMENTS

We are grateful to Maninder Heer and Maria Rigau for their critical comments. We thank Prof. Aristotelis Tsirigos for sharing their TAD insulation data. This work was supported by a Wellcome Trust (https://wellcome.ac.uk) Seed Award in Science (206103/Z/17/Z) awarded to D.R.

AUTHOR CONTRIBUTIONS

Conceptualization, C.J., M.T.-H., D.J., and D.R.; analysis, C.J., M.T.-H., and D.R.; writing, C.J., M.T.-H., D.J., and D.R.; supervision, D.J. and D.R.; funding acquisition, D.R.

DECLARATION OF INTERESTS

The authors declare no competing interests.

Received: August 20, 2022
Revised: November 3, 2023
Accepted: February 16, 2024

REFERENCES

1. Rada-Iglesias, A., Grosveld, F.G., and Papantonis, A. (2018). Forces driving the three-dimensional folding of eukaryotic genomes. Mol. Syst. Biol. *14*, e8214.
2. Stadhouders, R., Filion, G.J., and Graf, T. (2019). Transcription factors and 3D genome conformation in cell-fate decisions. Nature *569*, 345–354.
3. Krefting, J., Andrade-Navarro, M.A., and Ibn-Salem, J. (2018). Evolutionary stability of topologically associating domains is associated with conserved gene regulation. BMC Biol. *16*, 87.
4. Lazar, N.H., Nevonen, K.A., O'Connell, B., McCann, C., O'Neill, R.J., Green, R.E., Meyer, T.J., Okhovat, M., and Carbone, L. (2018). Epigenetic maintenance of topological domains in the highly rearranged gibbon genome. Genome Res. *28*, 983–997.
5. Liao, Y., Zhang, X., Chakraborty, M., and Emerson, J.J. (2021). Topologically associating domains and their role in the evolution of genome structure and function in. Genome Res. *31*, 397–410.
6. Ibn-Salem, J., Muro, E.M., and Andrade-Navarro, M.A. (2017). Co-regulation of paralog genes in the three-dimensional chromatin architecture. Nucleic Acids Res. *45*, 81–91.
7. Long, H.S., Greenaway, S., Powell, G., Mallon, A.-M., Lindgren, C.M., and Simon, M.M. (2022). Making sense of the linear genome, gene function and TADs. Epigenet. Chromatin *15*, 4.
8. Harmston, N., Ing-Simmons, E., Tan, G., Perry, M., Merkenschlager, M., and Lenhard, B. (2017). Topologically associating domains are ancient features that coincide with Metazoan clusters of extreme noncoding conservation. Nat. Commun. *8*, 441.
9. McArthur, E., and Capra, J.A. (2021). Topologically associating domain boundaries that are stable across diverse cell types are evolutionarily constrained and enriched for heritability. Am. J. Hum. Genet. *108*, 269–283.
10. Fudenberg, G., and Pollard, K.S. (2019). Chromatin features constrain structural variation across evolutionary timescales. Proc. Natl. Acad. Sci. USA *116*, 2175–2180.
11. Huynh, L., and Hormozdiari, F. (2019). TAD fusion score: discovery and ranking the contribution of deletions to genome structure. Genome Biol. *20*, 60.
12. Whalen, S., and Pollard, K.S. (2019). Most chromatin interactions are not in linkage disequilibrium. Genome Res. *29*, 334–343.
13. Canela, A., Maman, Y., Jung, S., Wong, N., Callen, E., Day, A., Kieffer-Kwon, K.-R., Pekowska, A., Zhang, H., Rao, S.S.P., et al. (2017). Genome Organization Drives Chromosome Fragility. Cell *170*, 507–521.e18.
14. Farré, M., Robinson, T.J., and Ruiz-Herrera, A. (2015). An Integrative Breakage Model of genome architecture, reshuffling and evolution: The Integrative Breakage Model of genome evolution, a novel multidisciplinary hypothesis for the study of genome plasticity. Bioessays *37*, 479–488.
15. Van de Peer, Y., Mizrachi, E., and Marchal, K. (2017). The evolutionary significance of polyploidy. Nat. Rev. Genet. *18*, 411–424.
16. Ohno, S. (1970). Evolution by Gene Duplication (Springer Berlin). https://doi.org/10.1007/978-3-642-86659-3.
17. Van de Peer, Y., Maere, S., and Meyer, A. (2009). The evolutionary significance of ancient genome duplications. Nat. Rev. Genet. *10*, 725–732.
18. Makino, T., and McLysaght, A. (2010). Ohnologs in the human genome are dosage balanced and frequently associated with disease. Proc. Natl. Acad. Sci. USA *107*, 9270–9274.
19. Sacerdot, C., Louis, A., Bon, C., Berthelot, C., and Roest Crollius, H. (2018). Chromosome evolution at the origin of the ancestral vertebrate genome. Genome Biol. *19*, 166.
20. Marlétaz, F., Firbas, P.N., Maeso, I., Tena, J.J., Bogdanovic, O., Perry, M., Wyatt, C.D.R., de la Calle-Mustienes, E., Bertrand, S., Burguera, D., et al. (2018). Amphioxus functional genomics and the origins of vertebrate gene regulation. Nature *564*, 64–70.
21. Capra, J.A., Stolzer, M., Durand, D., and Pollard, K.S. (2013). How old is my gene? Trends Genet. *29*, 659–668.
22. Capra, J.A., Stolzer, M., Durand, D., and Pollard, K.S. (2013). How old is my gene? Trends Genet. *29*, 659–668.

23. Domazet-Lošo, T., and Tautz, D. (2010). A phylogenetically based transcriptome age index mirrors ontogenetic divergence patterns. Nature *468*, 815–818.

24. Chen, W.-H., Trachana, K., Lercher, M.J., and Bork, P. (2012). Younger genes are less likely to be essential than older genes, and duplicates are less likely to be essential than singletons of the same age. Mol. Biol. Evol. *29*, 1703–1706.

25. Rancati, G., Moffat, J., Typas, A., and Pavelka, N. (2018). Emerging and evolving concepts in gene essentiality. Nat. Rev. Genet. *19*, 34–49.

26. Bartha, I., di Iulio, J., Venter, J.C., and Telenti, A. (2018). Human gene essentiality. Nat. Rev. Genet. *19*, 51–62.

27. Juan, D., Rico, D., Marques-Bonet, T., Fernández-Capetillo, O., and Valencia, A. (2014). Late-replicating CNVs as a source of new genes. Biol. Open *3*, 231.

28. Juan, D., Rico, D., Marques-Bonet, T., Fernández-Capetillo, O., and Valencia, A. (2013). Late-replicating CNVs as a source of new genes. Biol. Open *2*, 1402–1411.

29. Rigau, M., Juan, D., Valencia, A., and Rico, D. (2019). Intronic CNVs and gene expression variation in human populations. PLoS Genet. *15*, e1007902.

30. Herrero, J., Muffato, M., Beal, K., Fitzgerald, S., Gordon, L., Pignatelli, M., Vilella, A.J., Searle, S.M.J., Amode, R., Brent, S., et al. (2016). Ensembl comparative genomics resources. Database *2016*, 2016. https://doi.org/10.1093/database/bav096.

31. Ma, W., Ay, F., Lee, C., Gulsoy, G., Deng, X., Cook, S., Hesson, J., Cavanaugh, C., Ware, C.B., Krumm, A., et al. (2015). Fine-scale chromatin interaction maps reveal the cis-regulatory landscape of human lincRNA genes. Nat. Methods *12*, 71–78.

32. Martello, G., and Smith, A. (2014). The nature of embryonic stem cells. Annu. Rev. Cell Dev. Biol. *30*, 647–675.

33. Chakraborty, C., and Agoramoorthy, G. (2012). Stem cells in the light of evolution. Indian J. Med. Res. *135*, 813–819.

34. Agata, K., Nakajima, E., Funayama, N., Shibata, N., Saito, Y., and Umesono, Y. (2006). Two different evolutionary origins of stem cell systems and their molecular basis. Semin. Cell Dev. Biol. *17*, 503–509.

35. Zufferey, M., Tavernari, D., Oricchio, E., and Ciriello, G. (2018). Comparison of computational methods for the identification of topologically associating domains. Genome Biol. *19*, 217.

36. Rao, S.S.P., Huntley, M.H., Durand, N.C., Stamenova, E.K., Bochkov, I.D., Robinson, J.T., Sanborn, A.L., Machol, I., Omer, A.D., Lander, E.S., and Aiden, E.L. (2014). A 3D map of the human genome at kilobase resolution reveals principles of chromatin looping. Cell *159*, 1665–1680.

37. Javierre, B.M., Burren, O.S., Wilder, S.P., Kreuzhuber, R., Hill, S.M., Sewitz, S., Cairns, J., Wingett, S.W., Várnai, C., Thiecke, M.J., et al. (2016). Lineage-Specific Genome Architecture Links Enhancers and Non-coding Disease Variants to Target Gene Promoters. Cell *167*, 1369–1384.e19.

38. Bonev, B., Mendelson Cohen, N., Szabo, Q., Fritsch, L., Papadopoulos, G.L., Lubling, Y., Xu, X., Lv, X., Hugnot, J.-P., Tanay, A., and Cavalli, G. (2017). Multiscale 3D Genome Rewiring during Mouse Neural Development. Cell *171*, 557–572.e24.

39. Chang, L.-H., Ghosh, S., and Noordermeer, D. (2020). TADs and Their Borders: Free Movement or Building a Wall? J. Mol. Biol. *432*, 643–652.

40. Dixon, J.R., Selvaraj, S., Yue, F., Kim, A., Li, Y., Shen, Y., Hu, M., Liu, J.S., and Ren, B. (2012). Topological domains in mammalian genomes identified by analysis of chromatin interactions. Nature *485*, 376–380.

41. Cubeñas-Potts, C., and Corces, V.G. (2015). Topologically Associating Domains: An invariant framework or a dynamic scaffold? Nucleus *6*, 430–434.

42. Allou, L., and Mundlos, S. (2023). Disruption of regulatory domains and novel transcripts as disease-causing mechanisms. Bioessays *45*, e2300010.

43. Gong, Y., Lazaris, C., Sakellaropoulos, T., Lozano, A., Kambadur, P., Ntziachristos, P., Aifantis, I., and Tsirigos, A. (2018). Stratification of TAD boundaries reveals preferential insulation of super-enhancers by strong boundaries. Nat. Commun. *9*, 542.

44. Chen, W.-H., Lu, G., Chen, X., Zhao, X.-M., and Bork, P. (2017). OGEE v2: an update of the online gene essentiality database with special focus on differentially essential genes in human cancer cell lines. Nucleic Acids Res. *45*, D940–D944.

45. Schoenfelder, S., Furlan-Magaril, M., Mifsud, B., Tavares-Cadete, F., Sugar, R., Javierre, B.-M., Nagano, T., Katsman, Y., Sakthidevi, M., Wingett, S.W., et al. (2015). The pluripotent regulatory circuitry connecting promoters to their long-range interacting elements. Genome Res. *25*, 582–597.

46. Pancaldi, V., Carrillo-de-Santa-Pau, E., Javierre, B.M., Juan, D., Fraser, P., Spivakov, M., Valencia, A., and Rico, D. (2016). Integrating epigenomic data and 3D genomic structure with a new measure of chromatin assortativity. Genome Biol. *17*, 152.

47. Kalsoom, U.-e.-, Klopocki, E., Wasif, N., Tariq, M., Khan, S., Hecht, J., Krawitz, P., Mundlos, S., and Ahmad, W. (2013). Whole exome sequencing identified a novel zinc-finger gene ZNF141 associated with autosomal recessive postaxial polydactyly type A. J. Med. Genet. *50*, 47–53.

48. Xie, T., Yang, Q.-Y., Wang, X.-T., McLysaght, A., and Zhang, H.-Y. (2016). Spatial Colocalization of Human Ohnolog Pairs Acts to Maintain Dosage-Balance. Mol. Biol. Evol. *33*, 2368–2375.

49. Gaboriaud, J., and Wu, P.-Y.J. (2019). Insights into the Link between the Organization of DNA Replication and the Mutational Landscape. Genes *10*, 252. https://doi.org/10.3390/genes10040252.

50. Li, D., He, M., Tang, Q., Tian, S., Zhang, J., Li, Y., Wang, D., Jin, L., Ning, C., Zhu, W., et al. (2022). Comparative 3D genome architecture in vertebrates. BMC Biol. *20*, 99.

51. Álvarez-González, L., Burden, F., Doddamani, D., Malinverni, R., Leach, E., Marín-García, C., Marín-Gual, L., Gubern, A., Vara, C., Paytuví-Gallart, A., et al. (2022). 3D chromatin remodelling in the germ line modulates genome evolutionary plasticity. Nat. Commun. *13*, 2608.

52. Okhovat, M., VanCampen, J., Nevonen, K.A., Harshman, L., Li, W., Layman, C.E., Ward, S., Herrera, J., Wells, J., et al. (2023). TAD evolutionary and functional characterization reveals diversity in mammalian TAD boundary properties and function. Nat. Commun. *14*, 8111. https://doi.org/10.1038/s41467-023-43841-8.

53. Majic, P., and Payne, J.L. (2020). Enhancers Facilitate the Birth of De Novo Genes and Gene Integration into Regulatory Networks. Mol. Biol. Evol. *37*, 1165–1178.

54. Carelli, F.N., Liechti, A., Halbert, J., Warnefors, M., and Kaessmann, H. (2018). Repurposing of promoters and enhancers during mammalian evolution. Nat. Commun. *9*, 4066.

55. Davidson, B.S.A., Arcila-Galvis, J.E., Trevisan-Herraz, M., Mikulasova, A., Brackley, C.A., Russell, L.J., and Rico, D. (2023). The discovery of an evolutionarily conserved enhancer within the MYEOV locus suggests an unexpected role for this non-coding region in cancer. Preprint at bioRxiv. https://doi.org/10.1101/2023.09.18.558245.

56. Santiago-Algarra, D., Souaid, C., Singh, H., Dao, L.T.M., Hussain, S., Medina-Rivera, A., Ramirez-Navarro, L., Castro-Mondragon, J.A., Sadouni, N., Charbonnier, G., and Spicuglia, S. (2021). Epromoters function as a hub to recruit key transcription factors required for the inflammatory response. Nat. Commun. *12*, 6660.

57. Lewin, H.A., Richards, S., Lieberman Aiden, E., Allende, M.L., Archibald, J.M., Bálint, M., Barker, K.B., Baumgartner, B., Belov, K., Bertorelle, G., et al. (2022). The Earth BioGenome Project 2020: Starting the clock. Proc. Natl. Acad. Sci. USA *119*, e2115635118. https://doi.org/10.1073/pnas.2115635118.

58. Csárdi, G., Nepusz, T., Müller, K., Horvát, S., Traag, V., Zanini, F., and Noom, D. (2023). Igraph for R: R Interface of the Igraph Library for Graph

Theory and Network Analysis, Version 1.4.3 (Zenodo). https://doi.org/10.5281/ZENODO.7682609.

59. Durinck, S., Spellman, P., Birney, E., and Huber, W. (2009). Mapping identifiers for the integration of genomic datasets with the R/Bioconductor package biomaRt. Nat. Protoc. *4*, 1184–1191.

60. Durinck, S., Moreau, Y., Kasprzyk, A., Davis, S., De Moor, B., Brazma, A., and Huber, W. (2005). BioMart and Bioconductor: a powerful link between biological databases and microarray data analysis. Bioinformatics *21*, 3439–3440.

61. Wickham, H. (2016). ggplot2: Elegant Graphics for Data Analysis (Springer-Verlag New York).

CellPress
OPEN ACCESS

STAR★METHODS

KEY RESOURCES TABLE

REAGENT or RESOURCE	SOURCE	IDENTIFIER
Deposited data		
Human gene ages	This paper	https://github.com/ricolab/TAD_Evolution/blob/v1.0.0/data/Gene_Ages/Human/Ages.csv
Mouse gene ages	This paper	https://github.com/ricolab/TAD_Evolution/blob/v1.0.0/data/Gene_Ages/Mouse/MiceAges.txt
hESC DNase TADs	Ma et al.[31]	https://www.ncbi.nlm.nih.gov/geo/query/acc.cgi?acc=GSE56869 and https://github.com/ricolab/TAD_Evolution/blob/v1.0.0/data/TAD_maps/hESCTADs.tsv
mESC TADs	Bonev et al.[38]	https://www.ncbi.nlm.nih.gov/geo/query/acc.cgi?acc=GSE96107 and https://github.com/ricolab/TAD_Evolution/blob/v1.0.0/data/TAD_maps/mESCTADs.tsv
GM12878 original TADs	Rao et al.[36]	https://www.ncbi.nlm.nih.gov/geo/query/acc.cgi and https://github.com/ricolab/TAD_Evolution/blob/v1.0.0/data/TAD_maps/GSE63525_GM12878_primary%2Breplicate_Arrowhead_domainlist_sorted_noNested.txt
GM12878 redefined TADs with insulation scores	Gong et al.[43]	https://github.com/ricolab/TAD_Evolution/blob/v1.0.0/data/TAD_insulation/boundary-strength.tgz
TADs from monocytes	Javierre et al.[37]	https://osf.io/u8tzp/and https://github.com/ricolab/TAD_Evolution/blob/v1.0.0/data/TAD_maps/TADs_Mon_mean_merged.bed
TADs from neutrophils	Javierre et al.[37]	https://osf.io/u8tzp/and https://github.com/ricolab/TAD_Evolution/blob/v1.0.0/data/TAD_maps/TADs_Neu_mean_merged.bed
TADs from CD4 T cells	Javierre et al.[37]	https://osf.io/u8tzp/and https://github.com/ricolab/TAD_Evolution/blob/v1.0.0/data/TAD_maps/TADs_nCD4_mean_merged.bed
TAD boundary stability across cell types (100Kb)	McArthur and Capra[9]	https://github.com/emcarthur/TAD-stability-heritability/tree/master/data/boundariesByStability and https://github.com/ricolab/TAD_Evolution/tree/v1.0.0/data/TAD_stability_across_cell_types
Gene essentiality data	Chen et al.[44]	http://v2.ogee.info/browse/ and https://github.com/ricolab/TAD_Evolution/blob/v1.0.0/data/Gene_Essentiality/gene_essentiality.txt
PCHi-C - Human CD8 T cells	Javierre et al.[37]	https://osf.io/u8tzp/
PCHi-C - Mouse mESCs	Schoenfelder et al.[45]	EBI ArrayExpress: E-MTAB-2414 https://www.ebi.ac.uk/biostudies/arrayexpress/studies/E-MTAB-2414
Software and algorithms		
igraph	Csárdi et al.[58]	https://dx.doi.org/10.5281/zenodo.7682609
Gene age colocalization	This paper	https://github.com/ricolab/TAD_Evolution/tree/v1.0.0/colocalisation_pValues
biomaRt	Durinck et al.[59,60]	https://bioconductor.org/packages/release/bioc/html/biomaRt.html
ggplot2	Wickham,[61]	https://ggplot2.tidyverse.org/
Gene essentiality enrichments	This paper	https://github.com/ricolab/TAD_Evolution/tree/v1.0.0/TAD_Age_and_Essentiality_Analysis

RESOURCE AVAILABILITY

Lead contact

Further information and requests for resources should be directed to and will be fulfilled by the lead contact, Daniel Rico (daniel.rico@cabimer.es).

Materials availability

There are no newly generated materials associated with the paper.

Data and code availability

- This paper analyses existing, publicly available data. These accession numbers for the datasets are listed in the key resources table.
- All original code has been deposited at https://github.com/ricolab/TAD_Evolution and https://doi.org/10.5281/zenodo.10067329 and is publicly available as of the date of publication. DOIs are listed in the key resources table.
- Any additional information required to reanalyze the data reported in this paper is available from the lead contact upon request.

METHOD DETAILS

Dating ages in genes

An age was assigned to mouse and human genes using Ensembl (version 74) gene trees[30] as described before[28,29] and illustrated in Figures 1A and 1B. Our definition of gene age tries to date the last time a gene was involved in a gene birth event. In the case of genes that have been duplicated (according to the Ensembl trees, Figure 1B), we consider the node of their most recent duplication - accordingly, daughter genes will have the same age (if none of them are involved in more recent duplication). In the case of singleton genes (i.e., those without detectable duplicates), we consider their gene age as the last common ancestor of all species that have orthologs (Figure 1A). In other words, the gene age is the gene family birth event (see review by Capra and coworkers[21] about different ways to date gene ages).

The age groups Simiiformes, Catarrhini, Hominoidea, Hominidae, HomoPanGorilla and Homo sapiens were collapsed into Primate genes; while Rodent-specific merges Glires, Rodentia, Sciurognathi, Murinae and Mus musculus (here, we decided to name this group as Rodent because only the birth of 14 mouse genes were dated as Glires). Ten of the age groups correspond to the same ancestors in humans and mice (from Fungi-Metazoa to Eutheria) while the youngest group in each species corresponds to gene births that occurred in Primates (in humans) or Rodents (in mice).

The gene ages for human and mouse genes are available at https://github.com/ricolab/TAD_Evolution and https://doi.org/10.5281/zenodo.10067329 (key resources table).

TAD maps used in age co-localization analysis

For the gene age co-localization analysis (see quantification and statistical analysis) we used the TAD genomic coordinates as defined by the original papers: hESCs,[31] mESCs,[38] human GM12878 B-cell derived lymphoblastoid cells (original TADs[36] and TADs from Gong and co-workers[43]), monocytes, neutrophils and naive CD4 T cells (key resources table).[37] We only modified the original data from Rao et al.[36] to remove the nested TADs, as they would have given duplicated co-localizations. All the TADs used are available at are available at https://github.com/ricolab/TAD_Evolution and https://doi.org/10.5281/zenodo.10067329 (key resources table).

Gene essentiality data

Gene essentiality data from humans and mice was retrieved from OGEE database[44] (key resources table).

Promoter-capture HiC (PCHi-C) networks

Networks were constructed with igraph[58] R package from PCHiC data from mouse[45] and human cells[37] (key resources table) by considering genomic regions as nodes and physical interactions as edges.[46] We annotated each node with the genes and their ages. We created a subnetwork of young genes (Figure 1C), keeping interactions where at least one node contains a Primate or Rodent gene. Then, we grouped the nodes by gene and removed any duplicated edges so that each gene-gene interaction would only be represented once.

QUANTIFICATION AND STATISTICAL ANALYSIS

Gene age co-localization analysis

We generated the p value matrices by performing 100 randomizations to obtain the variance of the distribution of the probabilities to find each pair of gene ages within the same TAD (see Figure S1). Then, using the normal distribution, the p value was calculated as the probability of obtaining by chance alone the observed probability in the random distribution. We took as average the value of the null hypothesis, which was considered to be the probability of matching every age-pair without taking any TAD structure at all (considering the ages as being taken from a global pool rather than from any particular TAD). To facilitate the visualization of these p values, we calculated the natural cologarithm using a maximum value of 30. In order to differentiate between probabilities higher or lower than expected, the natural cologarithm (always positive since it is from a value lower than 1) was left unchanged (i.e., positive) if the probability of finding genes of an age pair together was higher than expected, or its sign was changed (becoming negative) for probabilities of finding a pair of ages lower than expected. The code to implement this is in function *getPairData*, available as part of the script *co-localisations_functions.R* at https://github.com/ricolab/TAD_Evolution and https://doi.org/10.5281/zenodo.10067329 (key resources table).

The same approach was used to do the co-localization analysis with fixed-size windows instead of TADs. The Euclidean distance between matrices was calculated with the dist() function in R.

TAD insulation

The insulation of TADs in GM12878 cells was calculated by averaging the two insulation scores of their boundaries, as calculated by Gong and co-workers.[43] Then, TADs were grouped into five groups of similar size based on their TAD insulation scores, from low to high insulation. The original TAD boundary insulation scores were kindly provided by Aristotelis Tsirigos and we made them publicly available with his permission at https://github.com/ricolab/TAD_Evolution and https://doi.org/10.5281/zenodo.10067329 (key resources table).

TAD stability across cell types

The stability of a TAD corresponds to the number of cell types where its boundaries are present. To study the stability of TADs across cell types, we used the TAD maps and associated stability scores calculated by McArthur and Capra[9] (key resources table). Their dataset includes definitions for 14,345 TAD boundaries and assigns to each of them a parameter, the stability percentile, that is associated with the number of cell types where it is present (which varies between one and 37). For example, if a TAD boundary is present in only one cell type, it corresponds to a stability percentile of 0.113175, but if it is present in 24 cell types, then its stability percentile is 0.901778. All TAD boundaries in this dataset span 100 kb.

We separated the dataset of TAD boundaries in two groups of approximately the same size depending on their presence in different cell types.

- the "stable" group, which was made of TAD boundaries present in five or more different cell types, including 7,509 TAD boundaries (52%).
- and the "unstable" group, which was made using the remaining 6,836 TAD boundaries (48%), present in less than five different cell types.
- For each of these two groups, we created a list of TADs as the region between two consecutive TAD boundaries by taking the central value between the beginning and end of each TAD boundary definition. In addition, we removed all the TADs that were nesting a TAD boundary from the other group (so that the final TAD definitions in either group were empty of other TAD boundaries). Using these criteria, we obtained two datasets:
- one with 4749 stable TADs, with an average length of 154 kb.
- another one with 4086 unstable TADs, with an average length of 268 kb.

For each of these two TAD groups, we calculated the percentage of old genes using our dataset of gene ages (taking into account our definition of "old gene", Figure 1C), defining as "old-depleted TADs" those that contained less than 10% of old genes. We observed that for the stable TADs, 323 out of 3031 had less than 10% of old genes (so the ratio corresponds to 0.1066), while for unstable TADs this filter is passed by 284 out of 1795 (ratio: 0.1582). This displays a higher amount of young TADs in unstable TADs. To assess the significance of this difference, we repeated the analysis 100 times for each group after randomizing the gene age labels. We observed that all the randomized cases fall in between these values (see Figure S6), therefore showing that this difference is indeed statistically significant. The data and code to reproduce the analysis is available at https://github.com/ricolab/TAD_Evolution and https://doi.org/10.5281/zenodo.10067329.

Enrichment of essential genes

The significance of the enrichments of essential genes in the different sub-groups of genes was calculated with Chi-squared tests using the chi.square() function in R, and the significance threshold was set at $p < 0.05$. The code to reproduce the analysis is available at https://github.com/ricolab/TAD_Evolution and https://doi.org/10.5281/zenodo.10067329.